

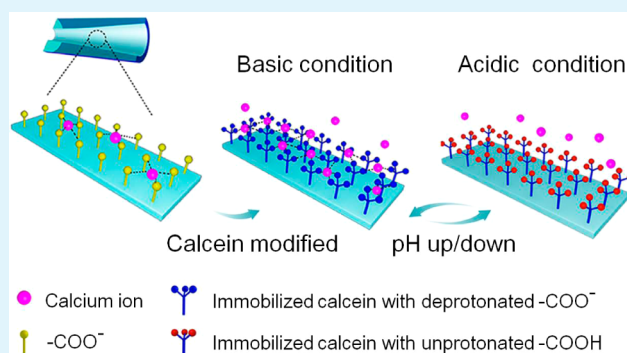
# Calcein-Modified Multinanochannels on PET Films for Calcium-Responsive Nanogating

Zheyi Meng, Chendi Jiang, Xiulin Li, and Jin Zhai\*

Key Laboratory of Bio-Inspired Smart Interfacial Science and Technology of Ministry of Education, School of Chemistry and Environment, Beihang University, Beijing 100191, P. R. China

## Supporting Information

**ABSTRACT:** Calcein-modified multiporous films with conical channels are introduced in a nanofluid device to enhance the calcium-responsive intensity and stability of ionic currents. Calcein with more carboxyls enhances the response of channels to calcium ions, and the capability of immobilized calcein for  $\text{Ca}^{2+}$ -binding could be regulated by the deprotonation of these carboxyls.



**KEYWORDS:** nanofluidics, calcium, nanoporous materials, biomimetics, ion channels

## INTRODUCTION

A crucial variety of calcium-dependent regulations through ion channels have been found in an extensive range of life processes,<sup>1–3</sup> like the functioning of nervous systems, the muscular contraction, the release of neurotransmitters and the cell proliferation. These biological ion channels contain constitutive or dissociable  $\text{Ca}^{2+}$ -responsive subunits composed by peptide fragments,<sup>4</sup> such as calmodulin, which supply binding sites for calcium ions. When calcium ions are chelated inside the ion channels, the ionic current through channels is blocked, and it results in the implementation of channel gating.<sup>5</sup> Enlightened by this mechanism, people have synthesized several artificial  $\text{Ca}^{2+}$ -responsive ion channels by applying materials with  $\text{Ca}^{2+}$ -binding sites as channels<sup>6,7</sup> or immobilized them on abiotic channel bases.<sup>8,9</sup> Compared with the biological counterparts embedding in fragile lipid bilayer membranes,<sup>10</sup> they are more mechanically robust in various surroundings. Viložny et al.<sup>8</sup> reported the reversible calcium ion response of protein-modified quartz nanopipettes. Siwy et al.<sup>6,7,11</sup> reported calcium-induced voltage gating, negative incremental resistance and oscillating ionic current through single conical nanopore prepared by track-etched polyethylene terephthalate (PET) films. Ali et al.<sup>9</sup> also utilized track-etched PET films in nanofluid device and reported calcium ion binding in a single conical nanopore functionalized with pH-responsive phosphonic polyacid chains. While the single channels of these studies render the small ionic currents vulnerable to noisy signals. A possible design to avoid these disadvantages is to utilizing multichannels,<sup>12,13</sup> which exert ionic transport equivalently with single ones but perform larger ionic conductance and less current fluctuations. However, multi-

channels have not been used in biomimetic ion-responsive nanogating devices yet.

Here, we introduce calcein-modified multiporous PET films with conical channels in a nanofluid device to enhance calcium-responsive intensity and stability of ionic currents. Carboxyl groups, which bind calcium ions as cations, are prepared on PET nanochannel walls by track-etching.<sup>14,15</sup> Deprotonation of surface carboxyls and binding of  $\text{Ca}^{2+}$  will change surface charge density, which influence ionic conductance of nanochannels.<sup>16,17</sup> So, calcium-binding could exert nanogating for ionic current through the channel. Calcein (2',7'-bis[N,N-bis(carboxymethyl)aminomethyl] fluorescein) is immobilized on the channel wall to enhance the response of the channel to  $\text{Ca}^{2+}$  (Scheme 1). It is a tetradentate ligand with four carboxyl groups, which could bind the calcium ion to form a chelate.<sup>18,19</sup> In our work, one carboxyl of calcein is used for immobilization with the PET channel, and the other three remain on the surface to supply more binding sites for  $\text{Ca}^{2+}$ . And the capability of immobilized calcein for  $\text{Ca}^{2+}$ -binding could be regulated by the deprotonation of the three carboxyls.

## RESULTS AND DISCUSSION

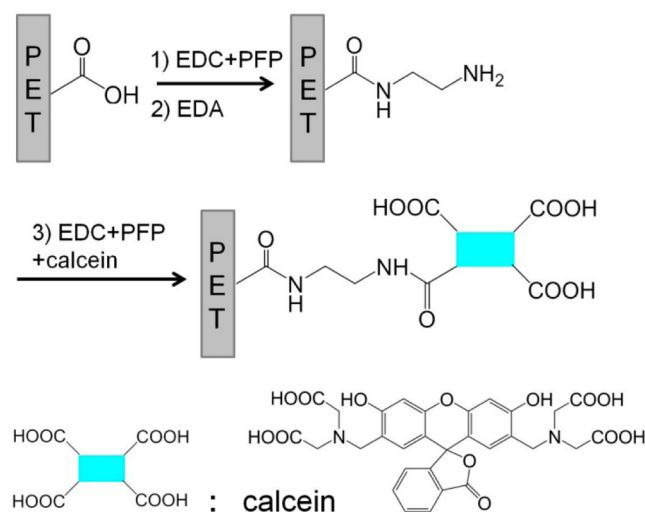
Conical PET multinanochannels were fabricated by the asymmetric ion-track etching, and the size of nanochannels was shown in Supporting Information 1. Calcein was modified on the channel surface by two steps (Scheme 1): first, a molecule of ethylenediamine (EDA) was immobilized with a

Received: January 14, 2014

Accepted: March 13, 2014

Published: March 13, 2014

Scheme 1. Attachment of Calcein on the Surface of the PET Nanochannels



carboxyl on the surface by one of its amino groups;<sup>20</sup> then, the EDA was attached with a calcein by the other amino. The success of the surface modification was verified by the corresponding current–voltage ( $I$ – $V$ ) curves measured at acid pH (details in Supporting Information 2). Ionic currents of multiple nanochannels were measured in an electrochemical conductivity cell, composed of two chambers, which were filled with identical electrolyte solution, separated by the PET multiporous film. The tip (the smaller opening) side of the channel was set as the negative pole of the bias. In Siwy's research,<sup>7,21</sup> the response to  $\text{Ca}^{2+}$  was performed by negative incremental resistance of the single channel (they also set the tip side as the negative pole). The binding of  $\text{Ca}^{2+}$  decreased the negative charge density on the surface, and it resulted in the decline of the ionic conductance. With the same responsive mechanism and setting of the negative pole, the response of our multichannels to  $\text{Ca}^{2+}$  can also be reflected by the negative incremental resistance. In our work, we choose the ionic current through multichannels under  $-2$  V ( $I_{-2V}$ ) for comparison. To avoid the precipitation of  $\text{Ca}^{2+}$  and phosphate,<sup>11,21</sup> we choose nonphosphate buffer solutions for different pH (glycine/KOH for pH 10, Tris/HCl for pH 7, acetic acid/KOH for pH 4).

Figure 1 shows the  $I$ – $V$  curves of calcein-modified and unmodified films in 0.1 M KCl solutions with/without 1 mM  $\text{CaCl}_2$  at basic pH. After modification,  $I_{-2V}$  declines 53.6% (here we only consider the magnitude of the current) with the presence of  $\text{Ca}^{2+}$ , from  $-317$  to  $-147$  nA, whereas the  $I_{-2V}$  of unmodified multichannels decreases just 40.8%, from  $-103$  to  $-61$  nA. And compared with single channels in previous researches, both multichannels conduct higher ionic currents under  $-2$  V in hundred nA scale.

The improvement of the response intensity to  $\text{Ca}^{2+}$  by the modification can be explained by the change of the surface charge<sup>17,22,23</sup> (Scheme 2). On the surface of the unmodified film, the number of  $-\text{COO}^-$  is limited, and they bind a few calcium ions. After modification, immobilized calcein supplies ample  $-\text{COO}^-$  for  $\text{Ca}^{2+}$ -binding. Calcium ions bound on the surface shield the negative charge of the wall, and the negative charge density declines significantly. It then weakens the voltage-dependent potential in the channel, which causes the decrease of the conductance under the negative voltage, or said

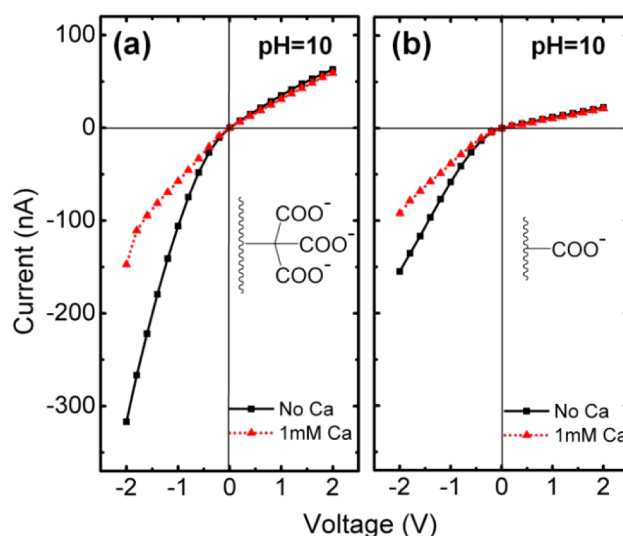
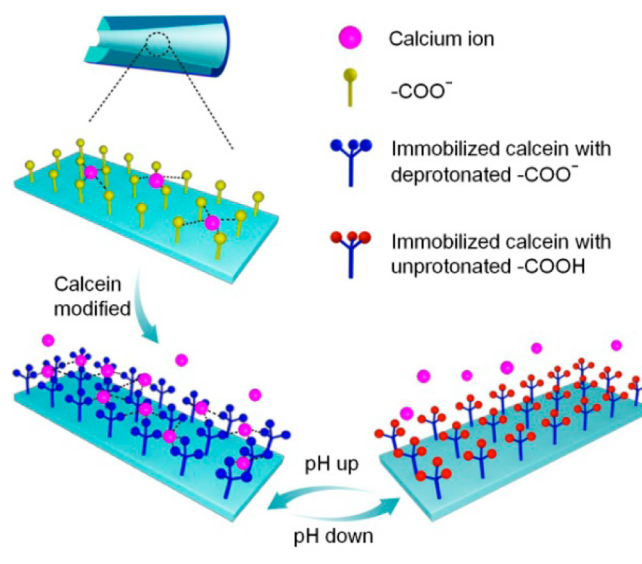


**Figure 1.**  $I$ – $V$  curves in 0.1 M KCl solution with (a) calcein-modified and (b) unmodified multichannels at pH 10. The solid line and the dot line were measured with the absence and the presence of 1 mM  $\text{CaCl}_2$ . The inner pictures in a briefly shows the immobilized calcein with three deprotonated carboxyls, and the one in b shows the deprotonated carboxyl on the unmodified surface.

**Scheme 2. Immobilized Calcein Increases the Intensity of Surface  $-\text{COO}^-$  (binding sites for  $\text{Ca}^{2+}$ ), and the Capability For  $\text{Ca}^{2+}$ -Binding Can Be Regulated by the Deprotonation of Calcein**



the negative incremental resistance. The Poisson/Nernst–Planck (PNP) model<sup>17,22,24</sup> was applied to support our explanation about the surface charge-dependent negative incremental resistance (Supporting Information 3). The theoretical ion distributions curves in the nanochannel along the pore axis (Figure 2a, b) shows that under the negative bias, the decrease of the negative charge density on the channel surface results in the decline of the local ionic concentrations in the channel along the pore axis, which could not supply ample ions for the ion current and inhibits the ionic transport. Here we choose from  $-3$  to  $-1$  e nm<sup>-2</sup>, because the density of the original carboxyls on the channel surface is about 1 nm<sup>-2</sup> and an immobilized calcein have three carboxyls. And it means the

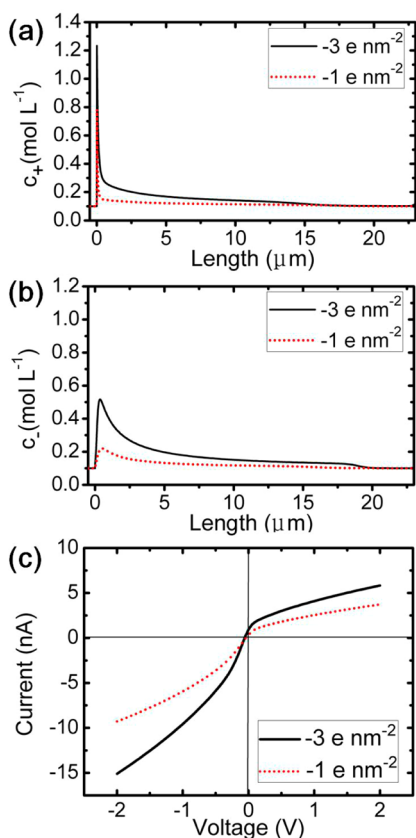


**Figure 2.** (a, b) Theoretical calculated (a) cation and (b) anion distribution curves under the bias of  $-2$  V in the conical channel with different surface charge densities (solid line,  $-3$  e nm $^{-2}$ ; dot line,  $-1$  e nm $^{-2}$ ). The tip side was considered as the zero point along the pore axis. (c) Theoretical  $I$ - $V$  curves with different surface charge densities (solid line,  $-3$  e nm $^{-2}$ ; dot line,  $-1$  e nm $^{-2}$ ). The contrary of the ionic currents under the negative voltage supported that the conductance of the channels will decline with the decreasing of the surface charge density.

negative incremental resistance is higher when the surface charges are less. The theoretical  $I$ - $V$  curves (Figure 2c) with different surface charge densities also verified the surface charge-dependent negative incremental resistance.

The modification of calcein not only improves the responsive intensity to  $\text{Ca}^{2+}$ , but also extends the responsive range to neutral pH. Figure 3 shows the  $I$ - $V$  curves of calcein-modified and unmodified films at neutral and acid pH. At pH 7 with the presence of 1 mM  $\text{CaCl}_2$ , the  $I_{-2V}$  of modified channels decreases 14.3% from  $-154$  to  $-132$  nA (Figure 3a). And at pH 4,  $I_{-2V}$  has no change with the absence/presence of  $\text{Ca}^{2+}$ . For unmodified channels, whether in the neutral or acid condition,  $I_{-2V}$  seems nearly the same with the absence/presence of  $\text{Ca}^{2+}$ .

The pH-dependent response of calcein-modified multichannels can be elucidated with the deprotonation of calcein by steps. In the aqueous solution,  $\text{pK}_a$  values of calcein at  $25$  °C are:  $\text{pK}_1 < 4$ ,  $\text{pK}_2$  5.4,  $\text{pK}_3$  9.0,  $\text{pK}_4$  10.5. At basic pH, the three  $-\text{COOH}$  are all protonated to  $-\text{COO}^-$ , and the response to  $\text{Ca}^{2+}$  is significant in this condition. For the neutral and acid condition, these  $-\text{COOH}$  are deprotonated incompletely, which results in insufficient binding sites for  $\text{Ca}^{2+}$  (Scheme 2).

The response of calcein-modified multiple channels and single channel are also compared. The preparation of the single

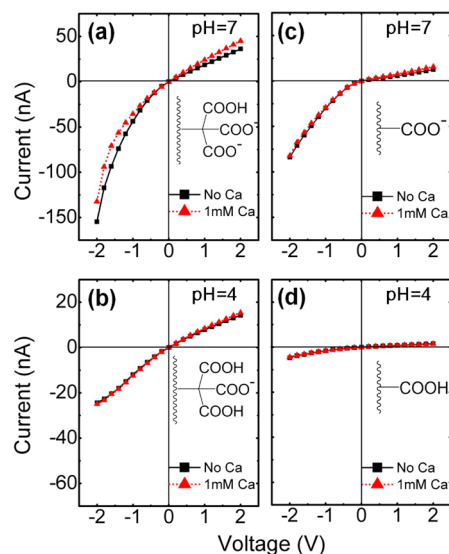


**Figure 3.**  $I$ - $V$  curves in 0.1 M KCl solution with (a, b) calcein-modified and (c, d) unmodified multichannels at pH 7 and 4. The solid line and the dot line were measured with the absence and the presence of 1 mM  $\text{CaCl}_2$ .

channel can be seen in the experimental section. Panels a and b in Figure 4 show  $I$ - $V$  curves of multiple and single channels

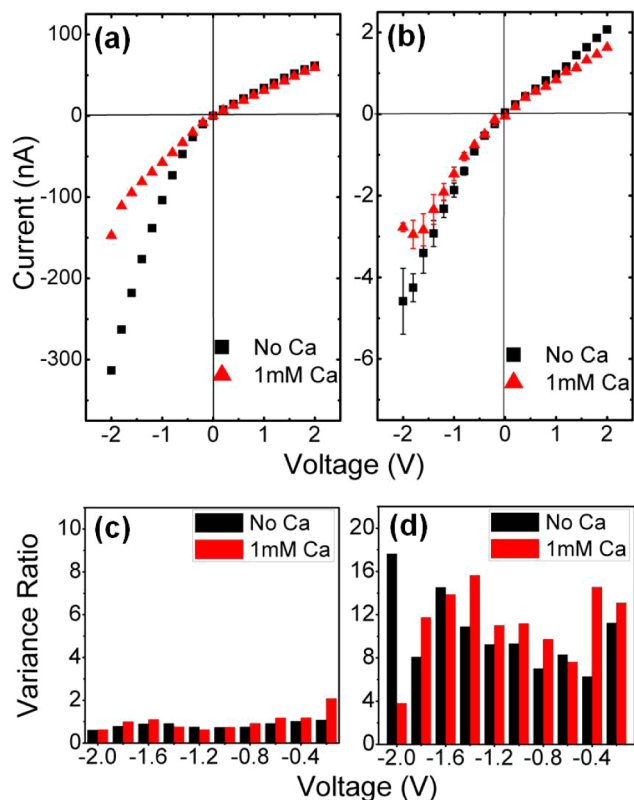


**Figure 4.** (a, b)  $I$ - $V$  curves in 0.1 M KCl solution with (a) modified multichannels and (b) single channel at pH 10. Square points and triangle points separately represent  $I$ - $V$  curves measured in the absence and the presence of 1 mM  $\text{CaCl}_2$ . Error bars reflect the standard deviation from five measurements in the same condition. (c, d) Variation ratio of the ionic current under negative voltage with (c) multiple and (d) single channels.

measured in 0.1 M KCl with/without 1 mM  $\text{CaCl}_2$  at pH 10. Error bars reflect the standard deviation from five measurements in the same condition. The response of the single nanochannel is relatively weaker than that of the multichannels, the  $I_{-2V}$  only declines 23.1% (from  $-4.59$  to  $-2.78$  nA) with the presence of 1 mM  $\text{Ca}^{2+}$  (Figure 4b), while the  $I_{-2V}$  of multiple ones drops 53.6%. On the other hand, the single channel performs larger standard deviations, and they are obvious in the  $I-V$  curves, whereas the error bars can be neglected in the  $I-V$  curves of the multiple ones. We choose the variation ratio (the ratio between the standard deviation value and the current value) with multiple and single channels under the negative voltage for more distinct comparison of the current stability. In Figure 3c, the variation ratio with them just distributes from 0.5 to 1%, which means the ionic current through multichannels is stable, whereas the current of the single one is more fluctuant and the variation ratio distributes from 8 to 12%. The comparison of the variation ratio under positive bias performs the same phenomenon, and it can be seen in Supporting Information 4.

The stability is due to the multiple structures. On one hand, multiple channels allow more ions to transfer through and conduct larger ionic current to reduce the influence of the noisy signal. On the other hand, the fluctuated currents in some channels can be averaged by those in other channels.

The responsible range of the calcium concentration is a crucial index to evaluate the sensing of a nanogating device. Figure 5a depicts the negative incremental conductance of

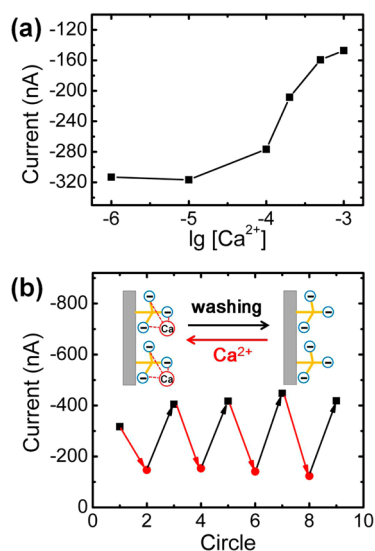


**Figure 5.** (a)  $\text{Ca}^{2+}$ -concentration-dependent  $I_{-2V}$  in 0.1 M KCl (pH10). (b) Reversibility of the response to  $\text{Ca}^{2+}$  with the modified multichannels.

modified multichannels with the presence of different  $\text{Ca}^{2+}$  concentrations in 0.1 M KCl solution at pH 10. With the decline of the  $\text{Ca}^{2+}$  concentration, the  $I_{-2V}$  of the multichannels drops gradually. At  $<1 \times 10^{-5}$  M, the  $I_{-2V}$  is nearly equal to the one with the absence of  $\text{Ca}^{2+}$ . So the sensing range of calcein-modified multichannel is  $\geq 1 \times 10^{-5}$  M. The concentration of  $\text{Ca}^{2+}$  more than 1 mM was not applied in our experiments to minimize the affection of  $\text{CaCl}_2$  to the conduction of the solution.<sup>25</sup>

There is one thing should be noticed that, the binding and unbinding of  $\text{Ca}^{2+}$  with calcein-modified multichannels are

reversible. The binding of  $\text{Ca}^{2+}$  with immobilized calcein in multichannels is also able to reappear for many times. Figure 5b illustrates that the  $I_{-2V}$  can be maintained in the same range in different  $\text{Ca}^{2+}$ -binding and washing circles.

## CONCLUSION

In a sum, we demonstrate the ionic transport performance of calcein-modified PET conical multinanochannels. We have found that attached calcein could enhance the response of channels to calcium ions and extend the responsive range, and compared to single channel, multichannels perform more obvious responsibility to calcium and higher stability of ionic current signals with a significant reduction in variation. The response of multichannels to  $\text{Ca}^{2+}$  is a reversible process and the responsive range is  $\geq 1 \times 10^{-5}$  M, which covers the  $\text{Ca}^{2+}$  concentration level in the blood of human and many other higher animals. With these advantages, we believe calcein-modified multiple nanochannels will have extensive applied potential in biomimetic nanogating devices and biosensors.<sup>26</sup>

## ASSOCIATED CONTENT

### Supporting Information

Experimental section, sizes of multiple and single conical PET nanochannels,  $I-V$  curves verifying the surface modification, the comparison of the variation ratio under positive voltage. This material is available free of charge via the Internet at <http://pubs.acs.org>.

## AUTHOR INFORMATION

### Corresponding Author

\*E-mail: zhajjin@buaa.edu.cn.

### Notes

The authors declare no competing financial interest.

## ACKNOWLEDGMENTS

We thank Dafeng Wang (PKU) for his linguistic improvements for our manuscript, and thank Jingtao Wang (BUAA) for theoretical calculations. This work is supported by the National Research Fund for Fundamental Key Projects (2011CB935704, 2012CB720904), National Natural Science Foundation (21271016) and Ph.D. Programs Foundation of Ministry of Education of China (30400002011127001).

## REFERENCES

- (1) Matulef, K.; Zagotta, W. N. Cyclic Nucleotide-Gated Ion Channels. *Annu. Rev. Cell Dev. Biol.* **2003**, *19*, 23–44.
- (2) Nonner, W.; Catacuzzeno, L.; Eisenberg, B. Binding and Selectivity in L-Type Calcium Channels: A Mean Spherical Approximation. *Biophys. J.* **2000**, *79*, 1976–1992.
- (3) Methfessel, C.; Boheim, G. The Gating of Single Calcium-Dependent Potassium Channels is Described by An Activation/Blockade Mechanism. *Biophys. Struct. Mech.* **1982**, *9*, 35–60.
- (4) Saimi, Y.; Kung, C. Calmodulin as An Ion Channel Subunit. *Annu. Rev. Physiol.* **2002**, *64*, 289–311.
- (5) Eismann, E.; Müller, F.; Heinemann, S. H.; Kaupp, U. B. A Single Negative Charge within The Pore Region of A CGMP-Gated Channel Controls Rectification,  $\text{Ca}^{2+}$  Blockage, and Ionic Selectivity. *Proc. Natl. Acad. Sci. U.S.A.* **1994**, *91*, 1109–1113.
- (6) Siwy, Z. S.; Powell, M. R.; Petrov, A.; Kalman, E.; Trautmann, C.; Eisenberg, R. S. Calcium-Induced Voltage Gating in Single Conical Nanopores. *Nano Lett.* **2006**, *6*, 1729–1734.
- (7) Siwy, Z. S.; Powell, M. R.; Kalman, E.; Astumian, R. D.; Eisenberg, R. S. Negative Incremental Resistance Induced by Calcium in Asymmetric Nanopores. *Nano Lett.* **2006**, *6*, 473–477.

- (8) Vilozny, B.; Actis, P.; Seger, R. A.; Vallmajo-Martin, Q.; Pourmand, N. Reversible Cation Response with a Protein-Modified Nanopipette. *Anal. Chem.* **2011**, *83*, 6121–6126.
- (9) Ali, M.; Nasir, S.; Ramirez, P.; Cervera, J.; Mafe, S.; Ensinger, W. Calcium Binding and Ionic Conduction in Single Conical Nanopores with Polyacid Chains: Model and Experiments. *ACS Nano* **2012**, *6*, 9247–9257.
- (10) García-Giménez, E.; Alcaraz, A.; Aguilera, V. M.; Ramírez, P. Directional Ion Selectivity in A Biological Nanopore with Bipolar Structure. *J. Membr. Sci.* **2009**, *331*, 137–142.
- (11) Powell, M. R.; Sullivan, M.; Vlasiouk, I.; Constantin, D.; Sudre, O.; Martens, C. C.; Eisenberg, R. S.; Siwy, Z. S. Nanoprecipitation-Assisted Ion Current Oscillations. *Nat. Nanotechnol.* **2008**, *3*, 51–57.
- (12) Liu, N.; Jiang, Y.; Zhou, Y.; Xia, F.; Guo, W.; Jiang, L. Two-Way Nanopore Sensing of Sequence-Specific Oligonucleotides and Small-Molecule Targets in Complex Matrices Using Integrated DNA Supersandwich Structures. *Angew. Chem., Int. Ed.* **2013**, *52*, 2007–2011.
- (13) Regonda, S.; Tian, R.; Gao, J.; Greene, S.; Ding, J.; Hu, W. Silicon Multi-Nanochannel FETs to Improve Device Uniformity/Stability and Femtomolar Detection of Insulin in Serum. *Biosens. Bioelectron.* **2013**, *45*, 245–251.
- (14) Siwy, Z.; Fuliński, A. Fabrication of a Synthetic Nanopore Ion Pump. *Phys. Rev. Lett.* **2002**, *89*, 198103.
- (15) Apel, P. Y.; Korchev, Y. E.; Siwy, Z.; Spohr, R.; Yoshida, M. Diode-Like Single-Ion Track Membrane Prepared by Electro-Stopping. *Nucl. Instrum. Methods Phys. Res., Sect. B* **2001**, *184*, 337–346.
- (16) Siwy, Z. S. Ion-Current Rectification in Nanopores and Nanotubes with Broken Symmetry. *Adv. Funct. Mater.* **2006**, *16*, 735–746.
- (17) Cervera, J.; Schiedt, B.; Neumann, R.; Mafe, S.; Ramirez, P. Ionic Conduction, Rectification, and Selectivity in Single Conical Nanopores. *J. Chem. Phys.* **2006**, *124*, 104706–9.
- (18) Saari, L. A.; Seitz, W. R. Immobilized Calcein for Metal Ion Preconcentration. *Anal. Chem.* **1984**, *56*, 810–813.
- (19) Diehl, H.; Ellingboe, J. L. Indicator for Titration of Calcium in Presence of Magnesium Using Disodium Dihydrogen Ethylenediamine Tetraacetate. *Anal. Chem.* **1956**, *28*, 882–884.
- (20) Nguyen, Q. H.; Ali, M.; Bayer, V.; Neumann, R.; Ensinger, W. Charge-Selective Transport of Organic and Protein Analytes through Synthetic Nanochannels. *Nanotechnology* **2010**, *21*, 365701.
- (21) Innes, L.; Powell, M. R.; Vlasiouk, I.; Martens, C.; Siwy, Z. S. Precipitation-Induced Voltage-Dependent Ion Current Fluctuations in Conical Nanopores. *J. Phys. Chem. C* **2010**, *114*, 8126–8134.
- (22) Cheng, L.-J.; Guo, L. J. Nanofluidic Diodes. *Chem. Soc. Rev.* **2010**, *39*, 923–938.
- (23) Schoch, R. B.; Han, J.; Renaud, P. Transport Phenomena in Nanofluidics. *Rev. Mod. Phys.* **2008**, *80*, 839–883.
- (24) Cervera, J.; Schiedt, B.; Ramirez, P. A Poisson/Nernst-Planck Model for Ionic Transport through Synthetic Conical Nanopores. *Europhys. Lett.* **2005**, *71*, 35–41.
- (25) Gillespie, D.; Boda, D.; He, Y.; Apel, P.; Siwy, Z. S. Synthetic Nanopores as A Test Case for Ion Channel Theories: The Anomalous Mole Fraction Effect without Single Filing. *Biophys. J.* **2008**, *95*, 609–619.
- (26) Hou, X.; Zhang, H.; Jiang, L. Building Bio-Inspired Artificial Functional Nanochannels: From Symmetric to Asymmetric Modification. *Angew. Chem., Int. Ed.* **2012**, *51*, 5296–5307.